Odd elasticity

Colin Scheibner,[1,2,*] Anton Souslov,[1,3,*] Debarghya Banerjee,[4,5]
Piotr Surówka,[6] William T. M. Irvine,[1,2,7] and Vincenzo Vitelli[1,2,†]

[1] *James Franck Institute, The University of Chicago, Chicago, Illinois 60637, USA*
[2] *Department of Physics, The University of Chicago, Chicago, Illinois 60637, USA*
[3] *Department of Physics, University of Bath, Bath BA2 7AY, United Kingdom*
[4] *Max Planck Institute for Dynamics and Self-Organization, 37077 Göttingen, Germany*
[5] *Instituut-Lorentz, Universiteit Leiden, Leiden 2300 RA, The Netherlands*
[6] *Max Planck Institute for the Physics of Complex Systems, 01187 Dresden, Germany*
[7] *Enrico Fermi Institute, The University of Chicago, Chicago, Illinois, 60637, USA*

A passive solid cannot do work on its surroundings through any quasistatic cycle of deformations [1, 2]. This constraint need not hold in active solids, to which energy is supplied by internal batteries, external fields, or biochemical sources [3–11]. Previous studies have elucidated how activity can dramatically modify the values of the elastic moduli [12–14] already present in passive elasticity. In this Letter, we show that static elastic moduli altogether absent in passive elasticity can arise from active, nonconservative microscopic interactions. These active moduli enter the antisymmetric (or odd) part of the static elastic modulus tensor and quantify the amount of work extracted along quasistatic strain cycles. In 2D isotropic media, two chiral odd-elastic moduli emerge in addition to the bulk and shear moduli. We discuss microscopic realizations that include networks of Hookean springs augmented with active transverse forces and non-reciprocal active hinges. Using coarse-grained microscopic models, numerical simulations, and continuum equations, we uncover phenomena ranging from auxetic behavior [14–18] induced by odd moduli to elastic wave propagation in overdamped media enabled by self-sustained active strain cycles. Our work sheds light on the non-Hermitian mechanics of two- and three-dimensional active solids that conserve linear momentum but exhibit a non-reciprocal [4, 19] linear response.

We begin with a simple microscopic view of odd elasticity. Fig. 1a shows a concrete illustration of an odd elastic solid as a network of masses connected by active bonds. Each bond contains two battery-powered propellers that blow air at a constant rate. When the spring inside the bond elongates (contracts), a gear system rotates the propellers to produce transverse forces proportional to the strain, see Supplementary Movie 1. For small strains, the force law is given by

$$\mathbf{F}(r) = (-k\hat{\mathbf{r}} + k^a\hat{\boldsymbol{\phi}})\ \delta r, \qquad (1)$$

* These authors contributed equally to this work.
† vitelli@uchicago.edu

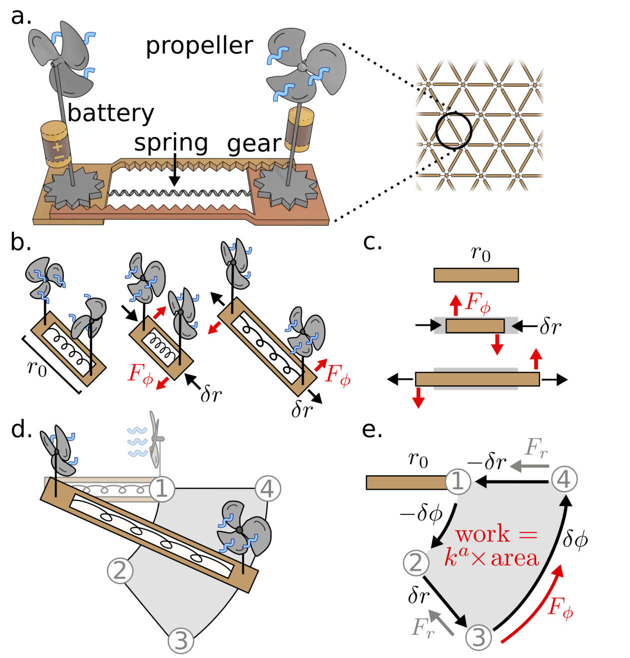

FIG. 1. **Quasistatic cycles with nonconservative interactions. a.** A mechanical realization of Eq. (1). Two propellers, mounted on platforms connected by a Hookean spring, are powered by batteries and blow air at a constant rate. As the platforms slide together or apart, a gear system rotates the propellers, giving rise to transverse forces. An elongated configuration is shown. A triangular lattice built out of such active bonds exhibits odd elasticity. **b-c.** When linearized, the bond gives rise to Eq. (1), which features an active transverse force (red arrows) proportional to strain (black arrows). (The Hookean spring provides a radial restoring force not shown.) This interaction is non-reciprocal: extension and compression induce torque, while rotation does not induce or relieve tension. Nonetheless, the interaction conserves linear momentum because the forces on each end of the bond are equal and opposite. **d-e.** When the bond is brought on a strain-controlled quasistatic cycle, the work done by the radial forces F_r on leg ①-② and leg ③-④ sums to zero. However, the transverse force F_ϕ does work on leg ②-③ that is not compensated for elsewhere on the cycle. For small angles $\delta\phi$ and strains $\delta r/r_0$, the work done by the bond on a quasistatic cycle is equal to k^a times the area enclosed.

where $\delta r = r - r_0$ is the radial displacement from the equilibrium length, r_0, and $\hat{\mathbf{r}}$ and $\hat{\boldsymbol{\phi}}$ are the unit vectors parallel and perpendicular to the bond, respectively. Eq. (1) describes a Hookean spring of spring constant k with an additional chiral, transverse force proportional to k^a, see Fig. 1b-c. At first sight, Eq. (1) seems merely to be a transverse generalization of Hooke's law. However, the non-vanishing $\boldsymbol{\nabla} \times \mathbf{F} = k^a$ implies that this pairwise force law is necessarily active. For small displacements, any (quasistatic) closed path will extract or inject a non-zero amount of energy or work $W = \oint \mathbf{F} \cdot \mathrm{d}\mathbf{l}$ equal (by Green's theorem) to k^a times the area enclosed, see Fig. 1d-e. While the example in Fig. 1 experiences a net torque in response to elongation or compression, this need not be the case if the active forces are *non-pairwise*. In the S.I., we present such a system using active hinges that do not require sources of angular momentum, yet still exhibit quasistatic path-dependent work. In both our microscopic models, the interactions share three crucial features: (i) they conserve linear momentum, (ii) they depend only on the relative positions of the particles, and (iii) they do not follow from a potential energy [12]. More realistic implementations of these active bonds and hinges may use piezoelectric components [20], robotic tentacles [21, 22], or mechanochemical interactions [23].

The microscopic units in Fig. 1, when connected in a network, violate one of the fundamental assumptions of classical elasticity: the existence of an elastic potential energy. Since the energetic state of each microscopic unit has quasistatic path dependence, the notion of an elastic potential energy is not well defined. Nonetheless, a stress-strain relation exists and can be linearized for small deformations. This approximation, known as Hooke's law, is captured by the equation $\sigma_{ij} = C_{ijmn} u_{mn}$, where u_{mn} are the gradients $\partial_m u_n$ of the displacement vector u_n, and C_{ijmn} is the elastic modulus tensor. In the absence of an elastic potential energy, the most general linear relationship between stress and displacement gradient for a two-dimensional isotropic solid reads:

$$\begin{pmatrix} \\ \\ \\ \\ \end{pmatrix} = \begin{pmatrix} B & 0 & 0 & 0 \\ A & 0 & 0 & 0 \\ 0 & 0 & \mu & K^o \\ 0 & 0 & -K^o & \mu \end{pmatrix} \begin{pmatrix} \\ \\ \\ \\ \end{pmatrix}, \qquad (2)$$

provided that no coupling to rotations is allowed, see Methods.

The notation in Eq. (2) is a geometric representation of Hooke's law $\sigma_{ij} = C_{ijmn} u_{mn}$. The displacement gradients on the right-hand side are decomposed along four independent components: dilation, rotation, and the two shear deformations S_1 and S_2, i.e. irreducible representations of SO(2). Similarly, the stress vector on the left-hand side is decomposed into pressure, torque, and the two shear stresses. Unlike passive isotropic media, the solid represented in Eq. (2) has four independent elastic moduli, not two. Besides the familiar bulk modulus, B, and shear modulus, μ, there are additional entries A and K^o. Qualitatively, the modulus A couples compression (and dilation) to an internal torque density, see Fig. 2a. By contrast, K^o does not entail a net torque density, but rather implies a 45° rotation between the applied shear strain and the resulting shear stress, see Fig. 2b. The asymmetry of the elastic modulus matrix in Eq. (2) implies a non-reciprocal, linear mechanical response, echoing the non-reciprocal linear response of a single bond in Fig. 1. In terms of microscopic parameters, we find $B = 2\mu = \frac{\sqrt{3}}{2} k$ and $A = 2K^o = \frac{\sqrt{3}}{2} k^a$ for a triangular lattice. As shown in the S.I., a honeycomb lattice with next-nearest-neighbor springs allows all four moduli to be tuned independently. Furthermore, we show that $A = 0$ identically for models based on active hinges rather than active springs, since the hinges do not require microscopic torques, see S.I.

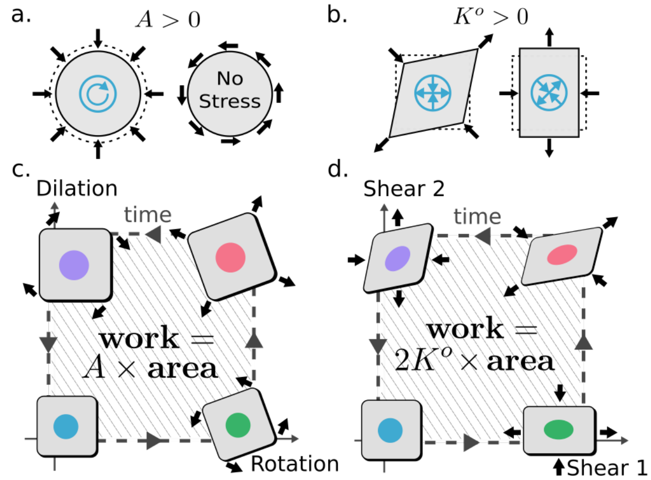

FIG. 2. **Odd elastic engine cycle.** **a.** The odd modulus A couples compression to an internal torque density, while rotations induce no stresses. The applied strains are represented by the black arrows, the undeformed shape by the dotted lines, and the internal stresses by the blue icons. **b.** The odd modulus K^o couples the two independent shear deformations. Unlike shear coupling in anisotropic passive solids, the induced stress is always rotated 45° counterclockwise relative to the applied strain. **c.** An odd elastic material is subjected to a closed cycle in deformation space. First, a counterclockwise rotation is followed by a volumetric strain ϵ_V, inducing a torque density $A\epsilon_V$. Next, the object does work $A\epsilon_V\epsilon_\theta$ on its surrounding as it is rotated clockwise through an angle ϵ_θ, before being compressed to its original size. The total work done is A times the area enclosed in deformation space: $\epsilon_V\epsilon_\theta$. **d.** An analogous cycle involving only shear stress and shear strain.

The moduli A and K^o violate the symmetry of the elastic modulus tensor $C_{ijmn} = C_{mnij}$, which applies whenever the stresses arise from gradients of a free energy $f = \frac{1}{2} C_{ijmn} u_{ij} u_{mn}$. Microscopic units with quasistatic path-dependent work, e.g. those in Fig. 1, can give rise to an additional contribution to the elastic modulus tensor: $C_{ijmn} = C^e_{ijmn} + C^o_{ijmn}$ with $C^o_{ijmn} = -C^o_{mnij}$, which we refer to as *odd* elasticity since it is antisymmetric (or odd) under exchange of the first and second pair of indices. For example, K^o and A are the additional moduli that arise when specialized to two-dimensional isotropic media. Such moduli are forbidden by energy conservation, but allowed in active media and metamaterials with nonconservative interactions. For example, the modulus K^o is compatible with broken microscopic time-reversal symmetry in active biological surfaces [24]. Odd elasticity is distinct from activity-induced negative compressibility [13, 14], which pertains only to the symmetric part of C_{ijmn}, and from viscous effects [2], which vanish in the quasistatic limit.

Both A and K^o are chiral, i.e. they describe a solid in which the action of a parity inversion is not equivalent to a rotation. Their chiralities are set by the sign of the induced torque and the direction of rotation between shear strain and shear stress, respectively. Here, chirality arises from activity, i.e. from the non-potential interactions, not from additional microscopic degrees of freedom, cf. passive Cosserat elasticity [25–27]. In the S.I., we show that anisotropic 2D odd elastic solids need not be chiral, and the elastic modulus tensor in 3D is always achiral irrespective of odd elasticity. A full classification of odd elasticity in 3D is obtained by decomposing the strain tensor using irreducible representations of SO(3), see S.I. A 3D odd elastic solid must necessarily be anisotropic and the elastic modulus tensor displays up to 36 additional moduli that cannot be derived from an elastic potential. Odd elasticity cannot exist in 1D, since the elastic modulus tensor is a scalar, which cannot be antisymmetric.

Since C^o_{ijmn} cannot be obtained from a free energy, an odd elastic solid may be taken through a closed cycle of quasistatic deformations with non-zero total work $\Delta w = \oint C^o_{ijmn} u_{mn} \mathrm{d}u_{ij}$ done by (or on) the material, as anticipated by the microscopic cycle shown in Fig. 1d-e. (See S.I. for a proof.) In Fig. 2c, we apply this general formula to a two-dimensional isotropic solid and illustrate such a cycle using rotations and dilations. The initial and final configurations are identical, hence, zero work is done by the conservative part C^e_{ijmn}. By contrast, the total work done due to the odd contribution C^o_{ijmn} is equal to the modulus A times the area enclosed by the cycle in the space of rotations and dilations. Fig. 2d shows an analogous cycle which involves only shear stress and shear strain. In 3D there are four independent cycles, see S.I. During an odd-elastic cycle, the energy generated or lost depends only on the geometry of the path through strain space and not on the strain *rate* $\dot{u}_{mn}$, in contrast to friction or dissipation, which always lead to energy *loss*. Other active solids like muscles do work by a different mechanism [28]: as they elongate and contract along the same path in strain space, their active stresses change according to chemical signals instead of strain. By contrast, stresses due to odd elasticity depend on strain alone, and the work extracted depends on the area enclosed in strain space.

To illustrate how odd elasticity compares to other manifestations of activity in solids, we write the linear active forces F^a_j in the following more general form (see Methods):

$$F^a_j = g_j(\mathbf{u}, \dot{\mathbf{u}}, \nabla \mathbf{u}, \dots) + \partial_i \big(C_{ijmn} u_{mn} + \eta_{ijmn} \dot{u}_{mn} \big). \tag{3}$$

The first term g_j summarizes non-viscoelastic active forces. These forces can be constant or explicitly proportional to displacement u_i, velocity $\dot{u}_i$, strain u_{ij} [4, 29, 30], strain rate $\dot{u}_{ij}$, or to fields other than u_i, such as temperature and electromagnetic fields [31, 32], or the nematic order parameter [5]. This term includes active body forces such as those exhibited by solids formed by self-propelled particles that manifestly violate conservation of linear momentum [33, 34]. The second term on the right-hand side of Eq. (3) captures the forces that result from the divergence of the viscoelastic stress tensor, i.e., from *two* spatial derivatives of displacement and velocity. It is well known that energy sources can renormalize the values of the passive elastic moduli or viscous coefficients that enter the symmetric part of C_{ijmn} or η_{ijmn} (e.g. negative compressibility [13, 14] and eddy viscosity [35]). Activity can also result in odd (or Hall) viscosity, which is the antisymmetric part of the viscosity tensor denoted by $\eta^o_{ijmn} = -\eta^o_{mnij}$ [36–40]. However, all the aforementioned effects are physically distinct from odd elasticity, which pertains to the antisymmetric part of C_{ijmn} and is a crucial, but previously absent, piece in presenting a unified picture of the phenomenology of linear active solids.

In the presence of odd elasticity, even the most familiar elastic phenomena appear in a new guise. Consider as an example, the Poisson's ratio $\nu \equiv -\frac{u_{xx}}{u_{yy}}$, i.e., the ratio between horizontal strain u_{xx} and vertical strain u_{yy} under uniaxial compression along $\hat{y}$. In absence of odd elasticity, the Poisson's ratio can be made negative by altering the bulk and shear moduli, B and μ, for example, via the geometry of microscopic structures [15–18] or energy flux [14]. Here, we focus on the effect of odd elasticity, which does not alter B and μ, but rather introduces additional elastic moduli.

Figure 3a shows the uniaxial compression of an odd elastic material having $K^o, B, \mu > 0$ and $A = 0$. In the S.I., we show that as $\left|\frac{2K^o}{B}\right|$ increases, the Poisson's ratio of a stable odd elastic solid approaches $\nu = -1$, the auxetic limit of stable passive solids. Moreover, an additional response, not observed in passive elasticity, emerges: the odd solid exhibits a horizontal deflection of the top surface with respect to the bottom surface, which we quantify via the odd ratio, $\nu^0 \equiv -\frac{u_{yx}}{2u_{yy}}$. Whereas in passive isotropic solids, the odd ratio is zero due to left-right symmetry, the odd shear coupling K^o manifestly breaks chiral symmetry and thus allows for deflection. In Fig. 3c, we plot analytical predictions for ν and ν^o as solid black lines. To validate our analytical results, we simulate a honeycomb lattice with nearest-neighbor and

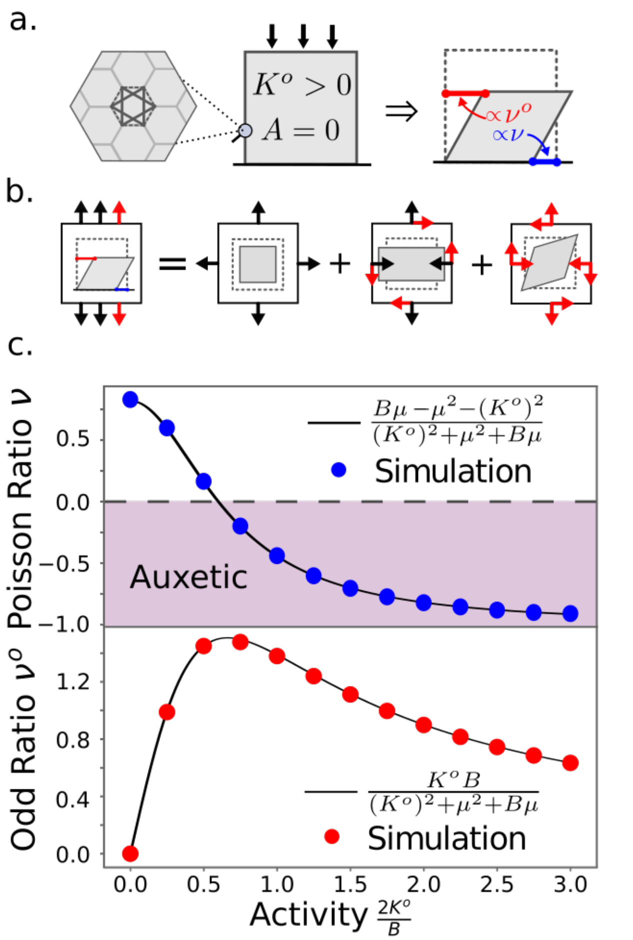

FIG. 3. **Statics in an odd elastic solid. a.** A honeycomb lattice with nearest-neighbor and next-nearest-neighbor odd springs can have $K^o > 0$ and $A = 0$ (and $B, \mu > 0$). When subject to uniaxial compression, such a solid responds by both net contraction [proportional to ν (blue)] and horizontal deflection [proportional to ν^o (red)]. **b.** Force balance in the uniaxial compression is shown schematically. Net strain can be decomposed into compression and shear in two directions. The resulting boundary stresses (arrows) cancel pressure on the top and bottom surfaces and maintain no stress on the sides. Black arrows show the response in the absence of odd elasticity, while the red arrows show the stresses due to K^o. **c.** Analytical calculations for the odd and Poisson's ratios with numerical validation. Simulations are performed using the honeycomb lattice, see S.I.

next-nearest-neighbor bonds. Using an analytic coarse-graining procedure (see S.I.), we obtain the values of K^o, μ, B, and A from the microscopic spring constants. The measured Poisson's ratio, plotted in Fig. 3c, agrees well with the prediction of the continuum theory without any fitting parameters.

Now we turn to odd elastodynamics. In passive materials, elastic waves cannot propagate when either (i) the bulk and shear moduli are vanishingly small $B = \mu = 0$ or (ii) the solid is overdamped. By contrast, odd elastic solids exhibit waves that propagate without any attenuation when both of these conditions are met because activity provides the energy to overcome dissipation in each wave cycle. Fig. 4a shows a snapshot of a plane wave traveling to the right in an overdamped solid in which $K^o \gg A, B, \mu$. (See Supplementary Movies 2 and 3.) The overdamped equation of motion is $\Gamma \dot{u}_j = \partial_i \sigma_{ij}$, where Γ is a friction coefficient with a substrate. (The momentum-conserving case of viscous damping, in which the dissipation is due to the relative velocity of solid particles, is treated in the S.I.) The colored ellipses in Fig. 4a (cf. Fig. 2c) represent the strain in regions bounded by the thick, black lines with the corresponding shear stresses shown in the row underneath. In Fig. 4b, we plot the stress and strain of a single deformed square as a function of time (indicated by color) in the space of shear S_1 and S_2. Fig. 4c-d show the analogous plots for a wave traveling in a 3D odd elastic medium. Shear stress and shear strain encode the basic mechanism for overdamped elastic wave propagation.

Fig. 4b illustrates two crucial features of waves in an overdamped odd elastic solid. First, stress and strain are $90°$ out of phase due to the antisymmetric shear coupling K^o. Thus, stress and strain in an overdamped odd elastic wave mimic the phase delay between strain and velocity that enables wave propagation in underdamped passive solids. Second, the trajectory of the wave in strain space traces out a circle. This circle indicates the emergence of an autonomous, self-sustaining elastic engine cycle, in which the system converts internal energy into mechanical work to offset dissipative losses [cf. Fig. 2c]. The speed of the wave can be deduced using a simple argument based on the balance of activity and dissipation. For a wave of amplitude R, an infinitesimal piece of material traces out a circle in strain space of radius qR, and so the energy injected due to activity is $2K^o \times \text{Area} = 2\pi K^o (qR)^2$. The energy loss due to dissipation in a single cycle is $\Gamma \times \text{velocity} \times (\text{distance traveled}) = 2\pi\Gamma\omega R^2$. Balancing the energy injected with the energy dissipated, one obtains the dispersion $\omega = K^o q^2/\Gamma$, and therefore the group velocity $\mathrm{d}\omega/\mathrm{d}q = 2K^o q/\Gamma$.

More generally, when B, μ, A and K^o are all nonzero, the equation of motion reads

$$-i\omega\Gamma \begin{pmatrix} u_\parallel \\ u_\perp \end{pmatrix} = q^2 \begin{pmatrix} B+\mu & K^o \\ -K^o - A & \mu \end{pmatrix} \begin{pmatrix} u_\parallel \\ u_\perp \end{pmatrix}, \tag{4}$$

where $u_\parallel$ is the longitudinal displacement and $u_\perp$ is the transverse displacement. To obtain the spectrum, we solve the secular equation corresponding to Eq. (4), see S.I. for the full expression. The active moduli enter the spectrum through the quantity $J = K^o(K^o + A)$. The qualitative behavior of the solid changes depending on whether J is above or below the threshold value $(B/2)^2$. For large J, waves propagate but attenuate exponentially with a rate proportional to $B/2 + \mu$. When J is smaller than the threshold, there is a sharp cutoff below which the real part of the spectrum vanishes, and no waves propagate. The phase diagram in Fig. 5a summarizes

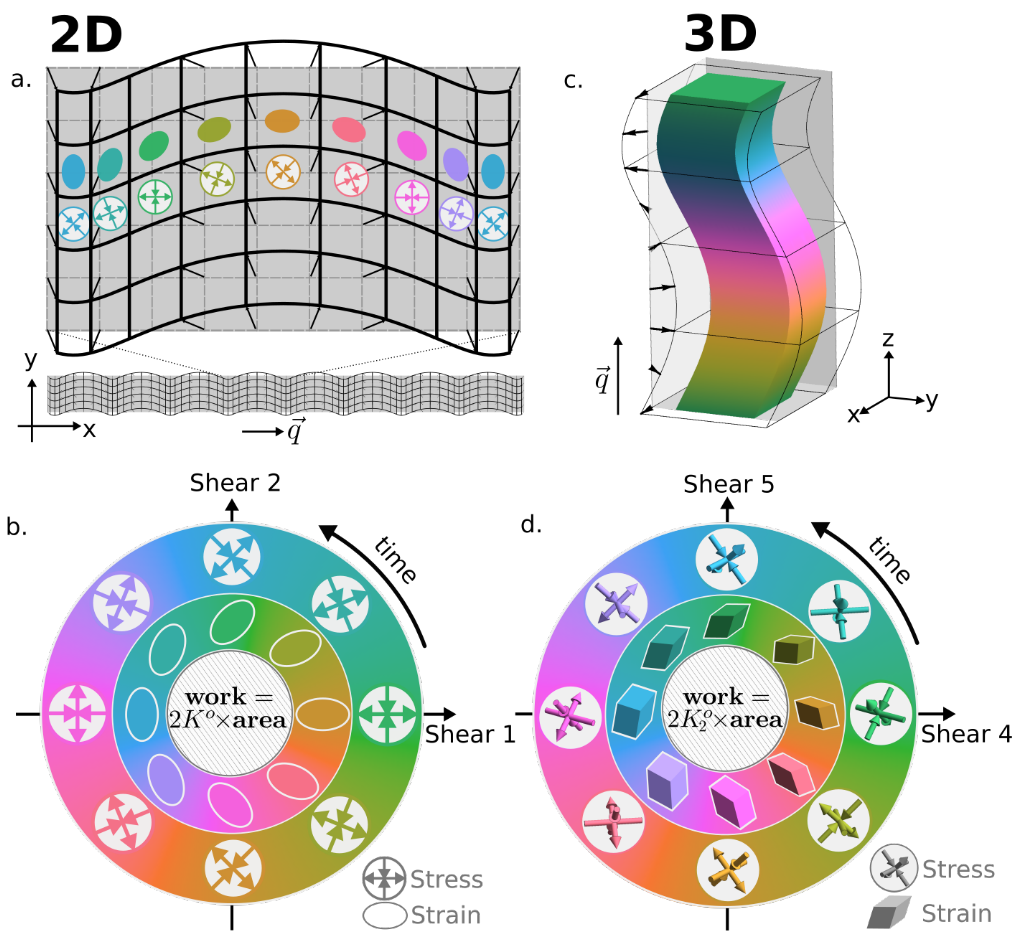

FIG. 4. **Odd elastic waves. a.** Real-space profile of an overdamped odd elastic wave traveling in the positive x-direction (for $K^o \gg A, B, \mu$). The light-grey background shows the undeformed material; the wave deforms the background grid into the thick black mesh. The ellipses illustrate the shear strain in a material patch and the disk-confined arrows represent the local shear stress. **b.** If a single material patch is tracked in time, the strain in the material traces out a circle in shear space. This circular trajectory encloses an area in strain space such that internal energy balances dissipative losses. The other essential ingredient for wave propagation is that stress and strain inside each patch are 90° out of phase (color represents time). (See Supplementary Movie 2.) **c.** A three-dimensional odd elastic wave traveling in a viscoelastic medium. The background gray represents the undeformed solid, while the colored interior and thin black frame represent a snapshot of the wave. The black arrows represent the displacement field and trace out a helix in the $\hat{z}$ direction. **d.** The cycle traced out by a single patch of material in strain space. The wave is powered by an odd elastic engine cycle in the space of shear 4 and shear 5, which are unique to three dimensions, see S.I.

the dynamic behavior of isotropic odd elastic solids, with the transition highlighted in red.

The matrix on the right-hand side of Eq. (4) times q^2 is known as the dynamical matrix. Since odd elasticity arises from linear, non-reciprocal interactions, the dynamical matrix is non-Hermitian. As illustrated in Fig. 5c and Supplementary Movie 4, the onset of odd-elastic waves displays characteristic features of non-Hermitian systems. In the absence of activity (●), the two eigenmodes are longitudinal and transverse. As activity increases, the eigenvectors are no longer orthogonal, and at the threshold $|k^a/k| = \frac{1}{\sqrt{3}}$, the eigenvectors are co-linear (★). The singularity caused by the degeneracy of the eigenvectors is a hallmark feature of non-Hermitian dynamics and is known as an exceptional point [41, 42]. Above the exceptional point (■), odd elastic waves propagate with circular polarization, tracing out a spiral in shear space due to attenuation. In the limit $|k^a/k| \gg 1$, the waves become self-sustaining and the spiral expands into an ellipse.

To understand the spectrum at shorter wavelengths, a microscopic structure must be specified. In Fig. 5b, we consider an unbounded triangular lattice of springs with conservative spring constant k and odd spring constant k^a. Analytic coarse graining shows that this microscopic realization corresponds to a position (set by k^a/k) on the dashed line in Fig. 5a. Elasticity describes the dynamics in the neighborhood of Γ, and the $\Gamma MK\Gamma$ cut in Fig. 5b shows how the wave-propagation threshold varies

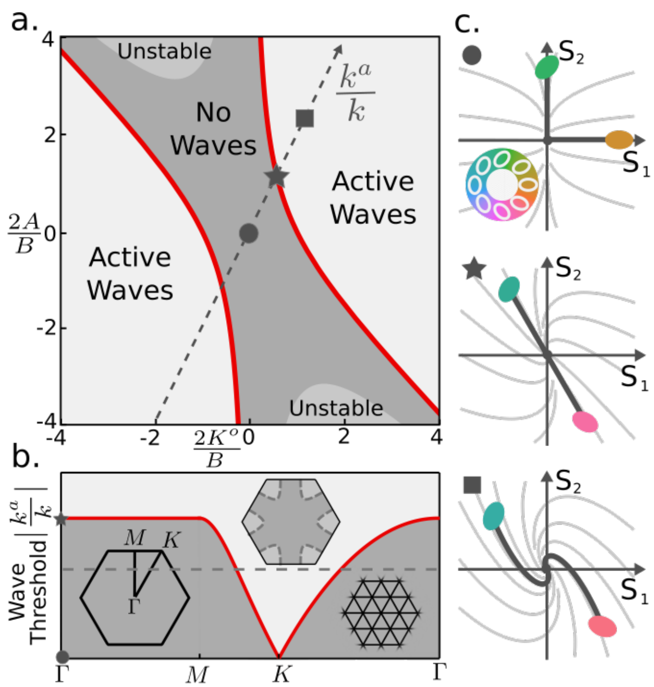

FIG. 5. **Exceptional points and non-Hermitian elastodynamics. a.** Phase diagram for waves in an overdamped odd elastic solid. Red curves represent the boundary outside of which active waves can be sustained. **b.** A cut ($\Gamma MK\Gamma$) through the space of wavevectors (first Brillioun zone) of a triangular lattice with generalized Hookean springs. The microscopic activity in the springs is characterized by the ratio $\left|\frac{k^a}{k}\right|$ between odd spring constant k^a and conservative spring constant k. The threshold for active waves varies across the Brilloin zone, with the elastic limit describing the region near Γ. The middle inset shows the regions of the Brillouin zone (light grey) in which waves propagate (for $\left|\frac{k^a}{k}\right|$ corresponding to the horizontal dashed line). **c.** The eigenmodes for three relative values of the elastic moduli, showing trajectories in shear space (S_1 and S_2, cf. Fig. 4). At zero activity (●), the modes correspond to longitudinal and transverse waves, whose eigenvectors are orthogonal in S_1-S_2 space. At the exceptional point (★), the eigenmodes become colinear. Above the exceptional point (■), the eigenmodes acquire a circular polarization, performing a spiral through simultaneous rotation and attenuation in strain space. (See Supplementary Movie 4.)

depending on the wavevector within the Brillouin zone. At zero activity, the spectrum of the triangular lattice is pierced by Dirac points at K and Γ. The exceptional points at K split into exceptional rings that flow outward. When $|k^a/k| = \frac{1}{\sqrt{3}}$ the exceptional points merge along the line ΓK and the bands open. The middle inset of Fig. 5b highlights the regions in the Brillouin zone (light grey) for which waves can propagate when, as an example, $\left|\frac{k^a}{k}\right|$ is given by the horizontal dashed line. The surprising feature is the existence of waves at short length scales well below the critical value in the continuum theory of Fig. 5a.

In summary, our work brings to light a neglected facet of linear elasticity in systems equipped with an internal source of energy. Future work will explore applications of odd elasticity to biomechanical systems [11, 24, 43, 44], kinematics of systems with transverse interactions such as gyroscopes or vortex lattices [45], viscoelastic quantum Hall states [46] and active metamaterials [4, 47] functioning as emergent soft robots that harvest energy, transmit it using odd mechanical waves, and perform work at designated sites. In addition, odd elasticity provides an alternative approach to design energy-absorbing materials that exploit quasistatic cycles instead of rate-dependent deformations.

Acknowledgments A.S., W.T.M.I., and V.V. acknowledge primary support through the Chicago MRSEC, funded by the NSF through grant DMR-1420709. C.S. was supported by the National Science Foundation Graduate Research Fellowship under Grant No. 1746045. W.T.M.I. acknowledges support from NSF EFRI NewLAW grant 1741685 and NSF DMR 1905974. P.S. was supported by the Deutsche Forschungsgemeinschaft via the Leibniz Program. We thank F. Jülicher and G. Salbreux for a critical reading of the manuscript.

I. METHODS

A. Elastic energy and symmetries of the elastic modulus tensor

The standard theory of elasticity begins with the postulation of an elastic free energy density f (see e.g., Ref. [1]). The free energy density is a function of the the displacement field u_i, which is the order parameter arising from the translational degrees of freedom of the microscopic constituents. The requirement that the elastic free energy be invariant under translations of the solid implies $\frac{\partial f}{\partial u_i} = 0$, so the free energy is only a function of gradients of u_j. In the limit of long-wavelength deformations, the lowest-order gradient $u_{ij} = \partial_i u_j$ dominates. Mechanical stability implies $\left.\frac{\partial f}{\partial u_{ij}}\right|_{u_{ij}=0} = 0$, so the lowest order term in strain must be quadratic. To linear order, the distances between points change only due to changes in the symmetrized displacement gradients $u^s_{ij} \equiv \frac{1}{2}(\partial_i u_j + \partial_j u_i)$. Therefore, u^s_{ij} defines the linear strain tensor, and the elastic free energy may be written as:

$$f = \frac{1}{2} K_{ijmn} u^s_{ij} u^s_{mn}, \tag{5}$$

where K_{ijmn} is a constant rank-4 tensor.

The stress tensor is given by:

$$\sigma^{\mathrm{eq}}_{ij} = \frac{\partial f}{\partial u^s_{ij}} = \frac{1}{2}(K_{ijmn} + K_{mnij}) u^s_{mn}. \tag{6}$$

Thus, we obtain the constitutive relation $\sigma_{ij}^{\mathrm{eq}} = C_{ijmn} u_{mn}^s$, where C_{ijmn} is known as the elastic modulus tensor. From Eq. (6) we see that

$$C_{ijmn} = \frac{1}{2}(K_{ijmn} + K_{mnij}) = C_{mnij}. \quad (7)$$

Therefore, if a solid medium obeys a linear constitutive relation which follows from a free energy, then the elastic modulus tensor must obey the major symmetry $C_{ijmn} = C_{mnij}$. Note that the definition $\sigma_{ij}^{\mathrm{eq}} \equiv \partial f / \partial u_{ij}^s$ implies that the stress is symmetric, $\sigma_{ij}^{\mathrm{eq}} = \sigma_{ji}^{\mathrm{eq}}$ (because u_{ij}^s is symmetric). In turn, this means that the non-active solid has no internal torques (evaluated as $\sigma_{ij}^{\mathrm{eq}} \epsilon_{ij} = 0$, where ϵ_{ij} is the two-dimensional Levi-Civita symbol).

In order to consider an odd elastic component $C_{ijmn}^o = -C_{mnij}^o$, we cannot start in the usual way from an elastic free energy. Instead, we begin from the constitutive relations directly: $\sigma_{ij} = C_{ijmn} u_{mn}^s$. If, unlike Eq. (6), the constitutive relations are not derived from an elastic free energy density, then an odd elastic component can exist. Materials with nonzero C_{ijmn}^o violate Maxwell-Betti reciprocity, i.e. mechanical reciprocity in their static response. Unlike Ref. [19], the non-reciprocity is present already in the linear response and relies on activity rather than non-linearities in the microscopic structure. Furthermore, the non-reciprocity due to C_{ijmn}^o is distinct from that observed in piezoelectrics [31, 32], which concerns the electromagnetic degrees of freedom, and from viscous effects, which exist only at finite frequency [2]. See S.I. Section J for more details.

B. Classification of elastic moduli

We now examine the basic features of linear elasticity in absence of an elastic potential energy. To begin, we suppose a solid body undergoes a deformation such that a point originally located at position $\mathbf{x}$ (having components x_i) ends up at location $X_i(\mathbf{x})$. We define the displacement vector field for the solid to be $u_i(\mathbf{x}) \equiv X_i(\mathbf{x}) - x_i$, and define the displacement gradient tensor to be $u_{ij}(\mathbf{x}) \equiv \partial_i u_j(\mathbf{x})$ (i.e., u_{ij} is related to the deformation gradient tensor $\Lambda_{ij} \equiv \partial X_i(\mathbf{x})/\partial x_j$ via $u_{ij} = \Lambda_{ij} - \delta_{ij}$, where δ_{ij} is the Kronecker-δ). Note that to linear order, u_{ij} plays the role of an unsymmetrized elastic strain tensor, which under the assumption of deformation dependence (see below) can be symmetrized in the usual way. The continuum version of Hooke's law postulates that if the displacement gradients are sufficiently small, the stress field $\sigma_{ij}(\mathbf{x})$ induced in a solid due to the displacement gradients is given by:

$$\sigma_{ij}(\mathbf{x}) = C_{ijmn} u_{mn}(\mathbf{x}), \quad (8)$$

where C_{ijmn} is known as the elastic modulus tensor. In what follows, we assume that the material is homogeneous, i.e., that C_{ijmn} is constant in space. The components of C_{ijmn} are known as elastic moduli, and they are the coefficients of proportionality between stress and strain that characterize the elastic behavior of a solid.

As we now show, basic assumptions about the interactions within the solid, such as conservation of angular momentum and conservation of energy, guarantee symmetries of the elastic modulus tensor. For convenience, we work in two dimensions and we introduce the following basis for 2×2 matrices:

$$\tau^0 = \begin{pmatrix} 1 & 0 \\ 0 & 1 \end{pmatrix} \quad (9)$$

$$\tau^1 = \begin{pmatrix} 0 & -1 \\ 1 & 0 \end{pmatrix} \quad (10)$$

$$\tau^2 = \begin{pmatrix} 1 & 0 \\ 0 & -1 \end{pmatrix} \quad (11)$$

$$\tau^3 = \begin{pmatrix} 0 & 1 \\ 1 & 0 \end{pmatrix}. \quad (12)$$

In this basis, we define:

$$u^0(\mathbf{x}) = \tau_{ij}^0 u_{ij}(\mathbf{x}) \qquad \text{Dilation} \quad (13)$$

$$u^1(\mathbf{x}) = \tau_{ij}^1 u_{ij}(\mathbf{x}) \qquad \text{Rotation} \quad (14)$$

$$u^2(\mathbf{x}) = \tau_{ij}^2 u_{ij}(\mathbf{x}) \qquad \text{Shear strain 1} \quad (15)$$

$$u^3(\mathbf{x}) = \tau_{ij}^3 u_{ij}(\mathbf{x}). \qquad \text{Shear strain 2} \quad (16)$$

These four independent components define the full displacement gradient tensor and can be interpreted as follows: u^0 measures the local, isotropic dilation of the solid. A dilation corresponds to change in area without change in shape or orientation; u^1 measures the local rotation, which corresponds to change in orientation without change in shape or area. Under transformations of 2D space, u^0 has the symmetry of a scalar and u^1 has the symmetry of a pseudo-scalar. The two components u^2 and u^3 define the shear strain, which corresponds to change in shape without change in area or orientation. Under rotations of 2D space, u^2 and u^3 both behave as bivectors, i.e., double-headed arrows. The space spanned by τ^2 and τ^3 is precisely that of symmetric traceless tensors. Specifically, u^2 measures shear strain with extension along the x-axis and contraction along the y-axis (or vice versa), which we dub shear 1 for convenience. On the other hand, u^3 measures shear 2, which has the axis of extension rotated 45° counterclockwise with respect to shear 1. Note that two independent shear vectors (in addition to compression and rotation) are needed to form a complete basis for arbitrary deformations.

We choose the same basis for the stress tensor:

$$\sigma^0(\mathbf{x}) = \tau_{ij}^0 \sigma_{ij}(\mathbf{x}) \qquad \text{Pressure} \quad (17)$$

$$\sigma^1(\mathbf{x}) = \tau_{ij}^1 \sigma_{ij}(\mathbf{x}) \qquad \text{Torque density} \quad (18)$$

$$\sigma^2(\mathbf{x}) = \tau_{ij}^2 \sigma_{ij}(\mathbf{x}) \qquad \text{Shear stress 1} \quad (19)$$

$$\sigma^3(\mathbf{x}) = \tau_{ij}^3 \sigma_{ij}(\mathbf{x}). \qquad \text{Shear stress 2} \quad (20)$$

The physical interpretation of these stresses are analogous to the strains: σ^0 is the (negative) of the isotropic pressure. The component σ^1 captures the antisymmetric part of the stress, i.e., the torque density. The two remaining components, σ^2 and σ^3, correspond to shear stresses.

In this notation, we express the elastic modulus tensor as a 4×4 matrix $C^{\alpha\beta} = \frac{1}{2}\tau^{\beta}_{ij} C_{ijmn} \tau^{\alpha}_{mn}$. Then Eq. (8) becomes:

$$\begin{pmatrix} \sigma^0(\mathbf{x}) \\ \sigma^1(\mathbf{x}) \\ \sigma^2(\mathbf{x}) \\ \sigma^3(\mathbf{x}) \end{pmatrix} = 2 \begin{pmatrix} C^{00} & C^{01} & C^{02} & C^{03} \\ C^{10} & C^{11} & C^{12} & C^{13} \\ C^{20} & C^{21} & C^{22} & C^{23} \\ C^{30} & C^{31} & C^{32} & C^{33} \end{pmatrix} \begin{pmatrix} u^0(\mathbf{x}) \\ u^1(\mathbf{x}) \\ u^2(\mathbf{x}) \\ u^3(\mathbf{x}) \end{pmatrix}. \tag{21}$$

Here, we review certain physical symmetries and conservation laws that constrain the form of $C^{\alpha\beta}$. The assumptions are stated independently and may be read in any order.

Deformation dependence (DD). A solid-body rotation of a material does not change the distance between points within that material (i.e., the metric). Therefore, one generally assumes that solid-body rotations do not induce stress, because stresses should only emerge if the object is deformed, not merely reoriented. This assumption is equivalent to the minor symmetry $C_{ijmn} = C_{ijnm}$, or in the notation of Eq. (21), $C^{\alpha 1} = 0$ for all α. Note that in our derivation, we use the displacement gradient tensor $u_{ij} \equiv \partial_i u_j$ instead of the linear symmetrized strain $u^s_{ij} \equiv \frac{1}{2}(\partial_i u_j + \partial_j u_i)$ or the full nonlinear strain tensor $u^{nl}_{ij} \equiv \frac{1}{2}(\Lambda_{ik}\Lambda_{kj} - \delta_{ij})$. The full tensor u^{nl}_{ij} is rotationally invariant at all orders, and at linear order reduces to u^s_{ij}. If C_{ijmn} has the minor symmetry $C_{ijmn} = C_{ijnm}$, then the product $C_{ijmn}u_{mn}$ is the same whether or not u_{mn} is symmetrized. We choose to work with the displacement gradient tensor u_{mn} (i.e., unsymmetrized strain) to be explicit about the assumption of non-coupling to rotation. Under DD alone, the elastic modulus tensor contains 12 independent moduli.

Isotropy (IS). Isotropy implies that the elastic modulus tensor remains unchanged through a rotation of the coordinate system. A passive rotation of the coordinate system through an angle θ maps $C^{\alpha\beta} \mapsto R^{\alpha\gamma}(\theta) C^{\gamma\sigma} R^{\beta\sigma}(\theta)$, where

$$R^{\gamma\sigma}(\theta) = \begin{pmatrix} 1 & 0 & 0 & 0 \\ 0 & 1 & 0 & 0 \\ 0 & 0 & \cos(2\theta) & \sin(2\theta) \\ 0 & 0 & -\sin(2\theta) & \cos(2\theta) \end{pmatrix}. \tag{22}$$

The requirement of isotropy can be restated as $C^{\alpha\beta} = R^{\alpha\gamma}(\theta) C^{\gamma\sigma} R^{\beta\sigma}(\theta)$ for all θ. Hence, under the assumption of isotropy alone, the most general form of the elastic modulus tensor is:

$$C^{\alpha\beta} = 2 \begin{pmatrix} C^{00} & C^{01} & 0 & 0 \\ C^{10} & C^{11} & 0 & 0 \\ 0 & 0 & C^{22} & C^{23} \\ 0 & 0 & -C^{23} & C^{22} \end{pmatrix}. \tag{23}$$

Therefore, under IS alone, the elastic modulus tensor has 6 independent moduli.

Conservation of energy (CE). Energy is fundamentally a conserved quantity. However, the constituents of a solid may have internal or external sources of energy that can be integrated out, resulting in phenomena which ostensibly violate energy conservation. In Section A of the S.I., we show that a elastic modulus tensor is compatible with an elastic potential if and only if $C_{ijmn} = C_{mnij}$. In the notation of Eq. (21), the condition for energy conservation is $C^{\alpha\beta} = C^{\beta\alpha}$. Under CE alone, the elastic modulus tensor contains 10 independent moduli.

Conservation of angular momentum (CAM). A material conserves angular momentum if it has no internal sources of torque. In this case, one requires that $\sigma_{ij} = \sigma_{ji}$, or equivalently $\sigma^1(\mathbf{x}) = 0$. To impose this constraint, one has to impose the left minor symmetry for the elastic modulus tensor $C_{ijmn} = C_{jimn}$, or in the notation of Eq. (21), $C^{1\alpha} = 0$ for all α. A medium with internal torques (generated, for example, by interactions with a substrate or internal spinning parts, see S.I.) may violate the symmetry of the stress tensor and therefore violate the left minor symmetry of the elastic modulus tensor. As with energy, angular momentum is a fundamentally conserved quantitiy, so any gain or loss of angular momentum must come from an internal or external angular momentum sink that has been integrated out of the analysis. Under CAM alone, the elastic modulus tensor has 12 independent moduli.

If deformation dependence is the only assumption present, then $C^{\alpha\beta}$ has 12 independent components. In the standard theory of linear elasticity with energy conservation, the number of independent components is reduced to 6. Note that when deformation dependence and energy conservation are both assumed, conservation of angular momentum is automatically implied because the left minor symmetry required for conservation of angular momentum is guaranteed by the right minor symmetry of deformation dependence in combination with the major symmetry associated with energy conservation. If one further assumes isotropy, the form of the elastic modulus tensor is restricted to have 2 independent components B and μ:

$$C^{\alpha\beta} = 2 \begin{pmatrix} B & 0 & 0 & 0 \\ 0 & 0 & 0 & 0 \\ 0 & 0 & \mu & 0 \\ 0 & 0 & 0 & \mu \end{pmatrix}. \tag{24}$$

Here, B is the familiar bulk modulus, which is the proportionality constant between compression and pressure; μ is the shear modulus, which is the proportionality constant between shear stress and shear strain.

In this work, we retain only deformation dependence and isotropy. We assume deformation dependence because stress only arises in the solids we consider as a result of relative displacements (i.e., changes in the material's metric). Note that isotropy is not a strict requirement, and many crystalline solids have anisotropic elastic modulus tensors. However, we consider only the isotropic case for simplicity. In this work we study odd elasticity, which arises when we lift the assumption of an elastic potential energy (i.e., conservation of energy). Assuming only isotropy and deformation dependence, the most general form of the elastic modulus tensor is

$$C^{\alpha\beta} = 2\begin{pmatrix} B & 0 & 0 & 0 \\ A & 0 & 0 & 0 \\ 0 & 0 & \mu & K^0 \\ 0 & 0 & -K^0 & \mu \end{pmatrix}. \tag{25}$$

In this case, there are two new moduli: A and K^o. As described in the text, A couples compression to internal torque density. The modulus K^o, like the shear modulus μ, is a proportionality constant between shear stress and shear strain. However, K^o mixes the two independent shears in an antisymmetric way.

Note that energy conservation is independent of angular-momentum conservation. We consider both cases: case (i), in which angular momentum is conserved and the solid has no internal torque density (i.e., $A = 0$) as well as case (ii) in which internal torques are present (i.e., $A \neq 0$). Even if $A = 0$, the modulus K^o can be nonzero. Hence, the existence of odd elasticity is not contingent on the presence of antisymmetric stress (or, equivalently, local torques).

In index notation, the most general form of the elastic modulus tensor from Eq. (25) is:

$$\begin{aligned} C_{ijmn} = B\delta_{ij}\delta_{mn} + \mu(\delta_{in}\delta_{jm} + \delta_{im}\delta_{jn} - \delta_{ij}\delta_{mn}) \\ + K^o E_{ijmn} - A\epsilon_{ij}\delta_{mn}, \end{aligned} \tag{26}$$

where

$$E_{ijmn} \equiv \frac{1}{2}(\epsilon_{im}\delta_{jn} + \epsilon_{in}\delta_{jm} + \epsilon_{jm}\delta_{in} + \epsilon_{jn}\delta_{im}). \tag{27}$$

We note that the decomposition in Eq. (2), and the analogous 3D expression, can also be used to classify the contributions to the viscosity tensor, with strain replaced by strain-rate, see S.I.

C. Odd elasticity in a general continuum framework for active solids

Odd elasticity is not a generic term for activity in solids, but rather a well-defined physical mechanism that generates active forces in solids or in other systems in which a generalized elasticity can be defined without using an elastic potential. In Section J of the S.I., we provide a detailed comparison between odd elasticity and other phenomena in solid mechanics. This section provides a justification for Eq. (3) and illustrates how odd elasticity fits into a larger continuum framework of active solids. A continuum theory of a solid describes the dynamics of the displacement field u_i along with a set of fields χ_α that represent additional degrees of freedom such as temperature, chemical concentration, electromagnetic fields, a nematic director, a microrotation field, etc. (Explicit examples are provided in Section J of the S.I.) We take the fields χ_α to be independent in that there is no constitutive relation allowing one field to be statically determined by the others.

The dynamics of the displacement field will be governed by the force density F_i, which we assume can be expanded in powers of χ_α and u_i (and their gradients) about a steady state or equilibrium value. We split the the forces into two contributions

$$F_i = F_i^\chi + F_i^d. \tag{28}$$

The F_i^χ are the forces which are proportional to χ_α or their derivatives. For example, in a piezoelectric solid with electric field E_k and piezoelectric tensor e_{ijk}, there is a contribution to the stress of the form $\sigma_{ij} = e_{ijk}E_k$, yielding a force term $f_j = e_{ijk}\partial_i E_k$ [31, 32]. In the case of active gels, the stress acquires a contribution of the form $\sigma_{ij} = \alpha Q_{ij}$, where Q_{ij} is the nematic order parameter and α is a constant [5]. See S.I. Section J for more detail and references.

The F_i^d captures all forces which are proportional to u_i or its derivatives. We assume the u_i and their gradients are small, so we retain only linear terms up to two derivatives in space and one derivative in time. The F_j^d may then be written as:

$$\begin{aligned} F_i^d =& (A_{ij} + B_{ij}\partial_t)u_j + (D_{ijk} + H_{ijk}\partial_t)\partial_j u_k \\ &+ (C_{ijmn} + \eta_{ijmn}\partial_t)\partial_j u_{mn}. \end{aligned} \tag{29}$$

The first two terms, proportional to A_{ij} and B_{ij}, physically represent, for example, pinning and substrate drag. The term proportional to D_{ijk} represents linear momentum exchange with a substrate, and has been considered in Refs. [4, 29, 30], see S.I., and is distinct from elasticity because the force is proportional to strain instead of gradients of strain. The final two terms represent linear viscoelasticity. The tensor η_{ijmn} is known as the viscosity tensor and relates stress to strain rate. The tensor C_{ijmn} is the elastic modulus tensor and relates stress directly to strain. All the tensor coefficients in Eq. (29) could in principle be functions of the χ_α. For example, in mechanocaloric solids and shape memory alloys, the elastic moduli are temperature dependent, see S.I. Furthermore, it has been shown that η_{ijmn} can acquire a nonzero antisymmetric part $\eta^o_{ijmn} = -\eta^o_{mnij}$, which is known as odd (or Hall) viscosity. All these effects are distinct from odd elasticity since odd elasticity refers to a nonzero antisymmetric part of C_{ijmn}, not merely a renormalization of the symmetric part of C_{ijmn}.

The quantity F_i^a in Eq. (3) in the main text illustrates many of the ways in which activity can manifest in continuum theories of solids. The term g_j includes the forces F_i^X and the first four terms of Eq. (29). The second term in Eq. (3) highlights explicitly the role of viscoelasticity. Our contribution in this work is to highlight that activity can introduce an antisymmetric part of the elastic modulus tensor and to explore its phenomenology and microscopic origins.

---

[1] Landau, L. *et al.* *Theory of Elasticity*. Course of theoretical physics (Elsevier Science, 1986).

[2] Lakes, R. *Viscoelastic Materials* (Cambridge University Press, 2009).

[3] Marchetti, M. C. *et al.* Hydrodynamics of soft active matter. *Reviews of Modern Physics* **85**, 1143–1189 (2013).

[4] Brandenbourger, M., Locsin, X., Lerner, E. & Coulais, C. Non-reciprocal robotic metamaterials. *Nature Communications* **10**, 4608 (2019).

[5] Prost, J., Jülicher, F. & Joanny, J. Active gel physics. *Nature Physics* **11**, 111 (2015).

[6] Lau, A. W. C., Hoffman, B. D., Davies, A., Crocker, J. C. & Lubensky, T. C. Microrheology, stress fluctuations, and active behavior of living cells. *Phys. Rev. Lett.* **91**, 198101 (2003).

[7] Maitra, A. & Ramaswamy, S. Oriented active solids (2018). arXiv:1812.01374.

[8] Hemingway, E. J. *et al.* Active viscoelastic matter: From bacterial drag reduction to turbulent solids. *Phys. Rev. Lett.* **114**, 098302 (2015).

[9] Murrell, M., Oakes, P. W., Lenz, M. & Gardel, M. L. Forcing cells into shape: the mechanics of actomyosin contractility. *Nature Reviews Molecular Cell Biology* **16**, 486 (2015).

[10] van Zuiden, B. C., Paulose, J., Irvine, W. T. M., Bartolo, D. & Vitelli, V. Spatiotemporal order and emergent edge currents in active spinner materials. *Proc. Natl. Acad. Sci. USA* **113**, 12919–12924 (2016).

[11] Needleman, D. & Dogic, Z. Active matter at the interface between materials science and cell biology. *Nature Reviews Materials* **2**, 17048 (2017).

[12] Thompson, J. M. T. 'paradoxical' mechanics under fluid flow. *Nature* **296**, 135–137 (1982).

[13] Lakes, R. Stable singular or negative stiffness systems in the presence of energy flux. *Philosophical Magazine Letters* **92**, 226–234 (2012).

[14] Lakes, R. & Wojciechowski, K. W. Negative compressibility, negative poisson's ratio, and stability. *physica status solidi (b)* **245**, 545–551 (2008).

[15] Lakes, R. Foam structures with a negative poisson's ratio. *Science* **235**, 1038–1040 (1987).

[16] Greaves, G. N., Greer, A. L., Lakes, R. S. & Rouxel, T. Poisson's ratio and modern materials. *Nature Materials* **10** (2011).

[17] Bertoldi, K., Reis, P. M., Willshaw, S. & Mullin, T. Negative poisson's ratio behavior induced by an elastic instability. *Advanced Materials* **22**, 361–366 (2010).

[18] Spadoni, A. & Ruzzene, M. Elasto-static micropolar behavior of a chiral auxetic lattice. *Journal of the Mechanics and Physics of Solids* **60**, 156 – 171 (2012).

[19] Coulais, C., Sounas, D. & Alù, A. Static non-reciprocity in mechanical metamaterials. *Nature* **542**, 461 (2017).

[20] Cui, H. *et al.* Three-dimensional printing of piezoelectric materials with designed anisotropy and directional response. *Nature Materials* **18**, 234–241 (2019).

[21] Polygerinos, P. *et al.* Soft robotics: Review of fluid-driven intrinsically soft devices; manufacturing, sensing, control, and applications in human-robot interaction. *Advanced Engineering Materials* **19**, 1700016 (2017).

[22] Roche, E. T. *et al.* A bioinspired soft actuated material. *Advanced Materials* **26**, 1200–1206 (2014).

[23] Katzir-Katchalsky, A. & Curran, P. *Nonequilibrium thermodynamics in biophysics*. Books in Biophysics (Harvard University Press, 1965).

[24] Salbreux, G. & Jülicher, F. Mechanics of active surfaces. *Phys. Rev. E* **96**, 032404 (2017).

[25] Eringen, A. C. *Microcontinuum field theories* (Springer, New York, 1999).

[26] Lakes, R. Elastic and viscoelastic behavior of chiral materials. *International Journal of Mechanical Sciences* **43**, 1579 – 1589 (2001).

[27] Frenzel, T., Kadic, M. & Wegener, M. Three-dimensional mechanical metamaterials with a twist. *Science* **358**, 1072–1074 (2017).

[28] Caruel, M. & Truskinovsky, L. Physics of muscle contraction. *Reports on Progress in Physics* **81**, 036602 (2018).

[29] Beatus, T., Tlusty, T. & Bar-Ziv, R. Phonons in a one-dimensional microfluidic crystal. *Nature Physics* **2**, 743–748 (2006).

[30] Beatus, T., Bar-Ziv, R. & Tlusty, T. Anomalous microfluidic phonons induced by the interplay of hydrodynamic screening and incompressibility. *Phys. Rev. Lett.* **99**, 124502 (2007).

[31] Lakes, R. Giant enhancement in effective piezoelectric sensitivity by pyroelectric coupling. *EPL (Europhysics Letters)* **98**, 47001 (2012).

[32] Faust, D. & Lakes, R. S. Reciprocity failure in piezoelectric polymer composite. *Physica Scripta* **90**, 085807 (2015).

[33] Protière, S., Couder, Y., Fort, E. & Boudaoud, A. The self-organization of capillary wave sources. *Journal of Physics: Condensed Matter* **17**, S3529–S3535 (2005).

[34] Lieber, S. I., Hendershott, M. C., Pattanaporkratana, A. & Maclennan, J. E. Self-organization of bouncing oil drops: Two-dimensional lattices and spinning clusters. *Phys. Rev. E* **75**, 056308 (2007).

[35] Starr, V. P. *Physics of negative viscosity phenomena*. Earth and planetary science series (McGraw-Hill, New York,, 1968).

[36] De Groot, S. R. *Non-equilibrium thermodynamics,* (North-Holland Pub. Co.; Interscience Publishers, Amsterdam, New York,, 1962).

[37] Avron, J. E. Odd Viscosity. *Journal of Statistical Physics* **92**, 543–557 (1998).

[38] Wiegmann, P. & Abanov, A. G. Anomalous hydrodynamics of two-dimensional vortex fluids. *Phys. Rev. Lett.* **113**, 034501 (2014).

[39] Banerjee, D., Souslov, A., Abanov, A. G. & Vitelli, V.

Odd viscosity in chiral active fluids. *Nature Communications* **8**, 1573 (2017).

[40] Soni, V. *et al.* The free surface of a colloidal chiral fluid: waves and instabilities from odd stress and hall viscosity (2018). arXiv:1812.09990v1.

[41] Bender, C. M. & Boettcher, S. Real spectra in non-hermitian hamiltonians having *pt* symmetry. *Phys. Rev. Lett.* **80**, 5243–5246 (1998).

[42] Heiss, W. The physics of exceptional points. *Journal of Physics A: Mathematical and Theoretical* **45**, 444016 (2012).

[43] Bi, D., Yang, X., Marchetti, M. C. & Manning, M. L. Motility-driven glass and jamming transitions in biological tissues. *Phys. Rev. X* **6**, 021011 (2016).

[44] Moshe, M., Bowick, M. J. & Marchetti, M. C. Geometric frustration and solid-solid transitions in model 2d tissue. *Phys. Rev. Lett.* **120**, 268105 (2018).

[45] Nash, L. M. *et al.* Topological mechanics of gyroscopic metamaterials. *Proc. Natl. Acad. Sci. USA* **112**, 14495–500 (2015).

[46] Offertaler, B. & Bradlyn, B. Viscoelastic response of quantum hall fluids in a tilted field. *Phys. Rev. B* **99**, 035427 (2019).

[47] Woodhouse, F. G., Ronellenfitsch, H. & Dunkel, J. Autonomous actuation of zero modes in mechanical networks far from equilibrium. *Phys. Rev. Lett.* **121**, 178001 (2018).